International Conference on Space Optics—ICSO 2012

Ajaccio, Corse

9–12 October 2012

Last results of MADRAS, a space active optics demonstrator

Marie Laslandes

Claire Hourtoule

Emmanuel Hugot

Marc Ferrari

et al.

Last results of MADRAS, a space active optics demonstrator

Marie Laslandes*, Claire Hourtoule*, Emmanuel Hugot*, Marc Ferrari*, Christophe Devilliers[†], Arnaud Liotard[†], Céline Lopez[‡] and Frederic Chazallet[§]

*Laboratoire d'Astrophysique de Marseille, CNRS and Aix Marseille Université, Marseille, France
[†]Thales Alenia Space, Cannes la Bocca, France
[‡]Thales SESO, Aix en Provence, France
[§]Shaktiware, Marseille, France

Email: marie.laslandes@oamp.fr

Abstract—The goal of the MADRAS project (Mirror Active, Deformable and Regulated for Applications in Space) is to highlight the interest of Active Optics for the next generation of space telescope and instrumentation. Wave-front errors in future space telescopes will mainly come from thermal dilatation and zero gravity, inducing large lightweight primary mirrors deformation. To compensate for these effects, a 24 actuators, 100 mm diameter deformable mirror has been designed to be inserted in a pupil relay. Within the project, such a system has been optimized, integrated and experimentally characterized. The system is designed considering wave-front errors expected in 3m-class primary mirrors, and taking into account space constraints such as compactness, low weight, low power consumption and mechanical strength. Finite Element Analysis allowed an optimization of the system in order to reach a precision of correction better than 10 nm rms. A dedicated test-bed has been designed to fully characterize the integrated mirror performance in representative conditions. The test set up is made of three main parts: a telescope aberrations generator, a correction loop with the MADRAS mirror and a Shack-Hartman wave-front sensor, and PSF imaging. In addition, Fizeau interferometry monitors the optical surface shape. We have developed and characterized an active optics system with a limited number of actuators and a design fitting space requirements. All the conducted tests tend to demonstrate the efficiency of such a system for a real-time, in situ wave-front. It would allow a significant improvement for future space telescopes optical performance while relaxing the specifications on the others components.

I. ACTIVE OPTICS IN THE SPACE CONTEXT

A. Use of active optics in astronomy

The purpose of active optics is to control mirrors' shape and deformation, and thereby the wave-front in optical instruments [1]. This control, at nanometrical precisions, makes possible the realization of high quality astronomical observations and facilitates the data reduction. Active optics is based on deformable mirrors, dedicated and optimized for specific needs. Allowing the use of very high optical quality components with complex shapes, variable or not, it presents many advantages and has various applications [2]. Three main fields of active optics can be defined: the maintaining of large mirrors optimal shapes [3], the in-situ correction of optical aberrations with active deformable mirrors [4] and the generation of aspherical

mirrors with stress polishing [5]. For about twenty years, active optics has allowed some technological breakthrough in astronomical instrumentation and is widely present on the large Earth-based telescopes. In this paper, we present the adaptation of active optics systems for future space observatories, dedicated to Earth or Universe study.

B. Evolution of space telescope and needs

Since their beginning, telescopes are evolving towards two main goals: increasing the collecting power and improving the angular resolution. These two characteristics directly depends on the optical aperture: access to finest observations would be possible with larger primary mirrors. However, the launch of space observatories imposes drastic constraints on satellites' weight and compactness. Thus, it becomes mandatory to use lightweight primary mirrors [6], [7]. Up to 3 meters, these mirrors can be contained in a rocket cap in one piece. For larger diameters, it will not be possible to use monolithic mirror with the actual rockets, segmented telescope concepts have to be adopted. Such as the James Webb Space Telescope, segmented systems could be launched folded and deployed in flight [8]. It is also envisaged to launch the instrument in separate pieces which would be assembled in flight [9].

Lightweight mirrors are sensitive to the environment variations, so the structure stability will become an important issue in telescopes' design. Thermal variation and absence of gravity will induce large mirrors' thermo-elastic deformations, generating optical aberrations in the instrument [10]. An active telescope would be then required in order to keep optimal performance. Active optics systems used in Earth-based telescopes are not directly applicable for space instrumentation. Considerations about weight, size, power consumption, mechanical strength and reliability has to be addressed. Two different approaches are under studies in order to compensate for these large lightweight mirrors deformations, privileging either the mirror weight or the system simplicity. The first solution consists in maintaining the primary mirror optimal shape with actuators under the optical surface, it requires an important number of actuators [11], [12]. The second solution

consists in performing the correction in a pupil relay, later in the optical train, it requires then a small active mirror with a limited number of actuators. While the first method is interesting for highly lightweight and flexible mirrors, the second one, simpler to carry out, is ideal for mirrors staying relatively rigid. A correcting mirror, designed for this second approach is presented in this paper.

C. MADRAS project

MADRAS (Miroir Actif Déformable et Régulé pour Applications Spatiales) is a collaborative project between Thales Alenia Space, Laboratoire d'Astrophysique de Marseille, Thales SESO and Shaktiware. It aims at developing a technological demonstrator of a correcting mirror for space telescopes.

As a study case, 3 meters class space telescopes are considered. Their expected primary mirror deformation are predicted thanks to telescopes' modeling and deformation datas from flying telescopes. It gives the specifications for the MADRAS mirror: the system has to correct the 9 Zernike modes defined in Table I, at amplitudes between 0 and 200 nm rms. The residual wave-front error after correction must be less than 5 nm rms for each modes separately and less than 10 nm rms for an actual wave-front error composed of a combination of these modes. Tip, tilt and focus are not addressed here, they will be corrected by a 5 degrees of freedom mechanism on the secondary mirror, adjusting the alignment. The correcting system addressing the effects of zero gravity and thermal dilatation, the required actuation frequency is low, the demonstrator works at 1 Hz.

The correcting system is designed taking into account space constraints. In order to have a light and compact system, the correction is done in a plane conjugated to the primary mirror, thus the aberrations generated by the large mirror deformation are compensated in a pupil relay of much more smaller dimensions. Considering 3-m class telescopes designs, the correcting mirror is 100 mm diameter, and the weight is limited to 5 kg. The system reliability and robustness are also studied: it is designed to survive space and launch environments.

The system performance are characterized in laboratory environment in order to improve its Technology Readiness Level to 4.

TABLE I
MODES TO CORRECT WITH MADRAS AND THEIR MAXIMUM
AMPLITUDES (TARGET PRECISION OF CORRECTION < 5 NM RMS).

Mode	Maximum amplitude (nm rms)
Coma3	200
Astigmatism3	150
Spherical3	50
Trefoil5	30
Astigmatism5	30
Tetrafoil7	30
Trefoil7	30
Pentafoil9	30
Tetrafoil9	30

II. PRESENTATION OF THE CORRECTING MIRROR

A. Mirror geometry

The chosen mirror geometry has been developed by Lemaitre [13]. It is a piece of Zerodur, made up of a circular pupil with an external thicker ring and 12 arms. The optical surface is deformed through 24 actuators applying discrete forces on either sides of each arm. In addition a central clamping is holding the system (Figure 1).

This design is based on the similarity between the Zernike polynomials used in the optical aberrations theory [14] and the Clebsch polynomials used in the elasticity theory [15]. It allows the generation of Zernike defined by $n = m$ and $n = m + 2$, n and m being the radial and azimuthal polynomials' orders. With 12 arms, m is included between 0 and 6. Furthermore, the central clamping allows the generation of the spherical aberration ($m = 0$ and $n = 4$).

In this design, forces to deform the mirror are applied far from the optical surface. This way, it avoids the generation of high spatial frequencies errors due to over-constraints at the force location, there is no actuator print-through. Moreover, it decouples the number of actuators from the mirror diameter: the number of required actuators is only driven by the maximal spatial frequency to be corrected. Finally, this design is not associated to one actuator technology: every actuator applying discrete forces can be used with this type of mirror.

B. Optimization with Finite Element Analysis

The mirror is in Zerodur, this material has been chosen for its low Coefficient of Thermal Expansion, ideal for a space use [16]. The system dimensions have been optimized in order to meet the correction specifications but also to ensure the system mechanical strength. The optimization is done with Finite Element Analysis and is based on the system Influence Functions (IF).

An Influence Function is defined as the wave-front resulting from the unit command on one actuator [17]. With 24 actuators, the studied system has 24 IF, constituting a characteristic base B which is used to decompose the wave-front error to correct ϕ_{in}:

$$\phi_{in} = B\alpha, \qquad (1)$$

with α a set of 24 coefficients corresponding to the actuators' commands.

These coefficients are determined by computing the generalized inverse of B:

$$\alpha = (B^t B)^{-1} B^t \phi_{in}. \qquad (2)$$

Thus, the wave-front actually compensated by the system is:

$$\phi_{cor} = B(B^t B)^{-1} B^t \phi_{in}, \qquad (3)$$

and the residual wave-front after correction:

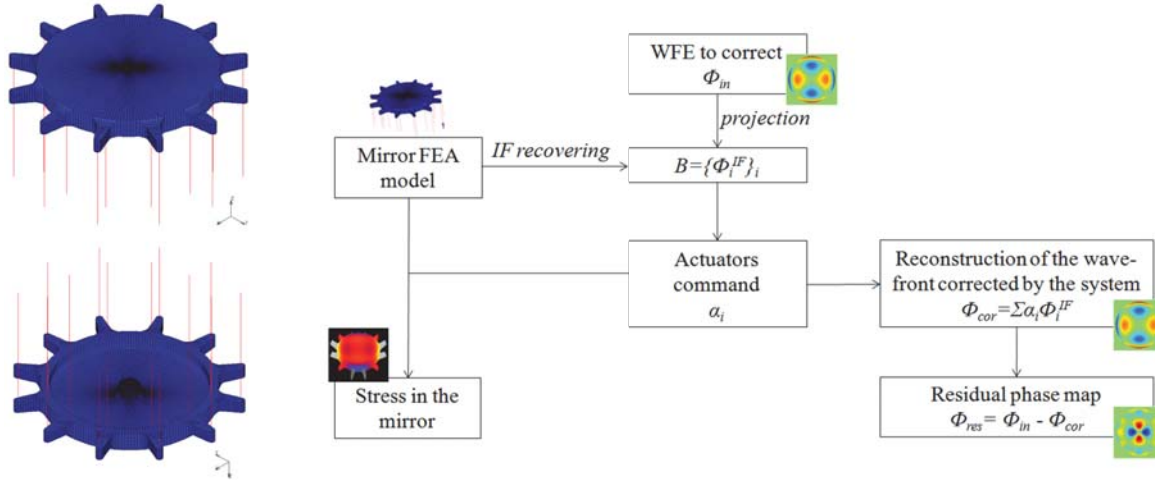$$\phi_{out} = \phi_{in} - \phi_{cor}. \qquad (4)$$

Fig. 1.   Left: Finite Element Model of the MADRAS mirror (actuator are represented by springs, in red) - 63708 hexaedrical elements, 77979 nodes - Right: Method for design optimization, based on the finite element model's influence functions: the three minimized criterions are the stress in the mirror, the actuators commands and the residual wave-front error.

For a given geometry, a Finite Element model is created and the Influence Functions are recovered by applying a unit displacement at each actuator location, while the other are fixed. Then, as described in Figure 1, the generation of the 9 specified Zernike modes is characterized by determining:
- the actuators' commands α with the projection of the mode on the IF base (Eq. 2),
- the residues of correction ϕ_{out} with the reconstruction of the corrected wave-front (Eq. 4),
- the resulting stress σ with the injection of the actuators commands on the finite element model.
The goal of the optimization is to minimize these 3 criterions for each specified mode. A classical least square algorithm is used to converge to the optimal geometry. The optimization output parameters are the pupil thickness, the outer ring dimensions (thickness and diameter) and the arms dimensions (thickness and length). A coefficient β_i is allocated to each mode according to its maximum amplitude to be corrected (Table I): Coma, Astigmatism and Spherical modes have more weight in the optimization. At the end, the quantity minimized by the least square algorithm is γ:

$$\gamma(geometry) = \sum_i \beta_i[||\phi_{out}||^2 + \sigma_{max} + \alpha_{max}], \quad (5)$$

with i varying from 1 to 9, representing the specified Zernike modes.

Once the optimal system geometry is defined, the mechanical and optical behavior is fully characterized with FEA. The precision of correction (ϕ_{out}) is known for each modes, such as the required actuators' stroke (α) and the level of stress in the mirror (σ). The worst case study allows the system validation : it consists in the correction of all the specified mode at their maximum amplitude, in the same time and orientation. In such a case, the characteristics computed for each modes are added. The expected precision of correction

is then 10.2 nm rms, for a specification at 10 nm rms. The maximum level of stress in the Zerodur is expected at 5 MPa, for an elastic limit at 10 MPa. Both values are acceptable. This study also gives the maximum actuators' required stroke, 6.8 μm, which would drive the actuators choice.

C. Integrated system

The correcting system is composed of three main parts: the mirror in Zerodur, the supporting structure in Invar and the 24 actuators. The overall system weighs 4 kg and is 80 mm height, for a diameter of 130 mm. As seen in the previous section, the mirror geometry has been optimized with Finite Element Analysis. The pupil diameter is 90 mm, for a thickness of 3.5 mm. The mirror is held on its center by a cone, linked to a rigid reference plate. The 24 actuators are clamped between the mirror's arms and the reference plate. They are piezoelectrical PZT chosen to have the stroke specified by FEA results: they can apply ± 10 μm displacement, with a maximum voltage of 80 V. They are connected with a proximity electronics which is wired to an electronic housing. To finish, the system is clamped on a tip/tilt plate with three bipods. This fixation device has been designed in order not to stress the system.
Except for the electronics, the entire system is designed for a space use. The entire system is modeled with FEA, in order to verify that the structure does not change the correcting performance or the mirror mechanical behavior. A dynamic analysis is also performed to simulate the launch vibration.

III. INTERFEROMETRICAL TESTS

Once the system is designed and integrated, a first round of test is conducted with a Fizeau interferometer, directly measuring the optical surface deformation. The mirror is tested horizontally, facing down, because it is the best configuration regarding gravity effects.
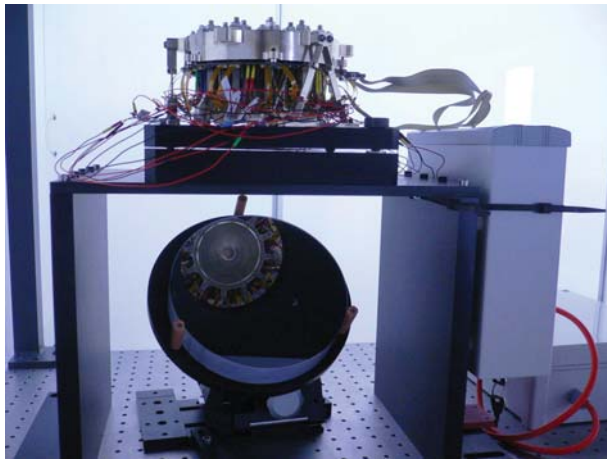
Fig. 2. Integrated system on its test platform.

Fig. 4. Difference between simulated and measured Influence Functions (on normalized maps)

A. Influence functions and eigen modes

The 24 system's Influence Function are measured by applying a push pull to each actuator while the other are at rest. The recovered IF (Figure 3) are compared to the ones expected from FEA. As we can see in Figure 4, their shapes are really similar. The only notable difference comes from their amplitudes: the ratio between internal and external IF is two times smaller on the measurements than on the simulation. This probably comes from the fact that the internal actuators are more constrained so their effect is minimized. This will not limit the mirror functioning because the stroke required for the internal actuators is small compared to the actuators available stroke.

The system eigen modes are determined by performing a Singular Value Decomposition on the IF base. As we can see in Figure 5, the eigen modes are well similar to Zernike polynomials.
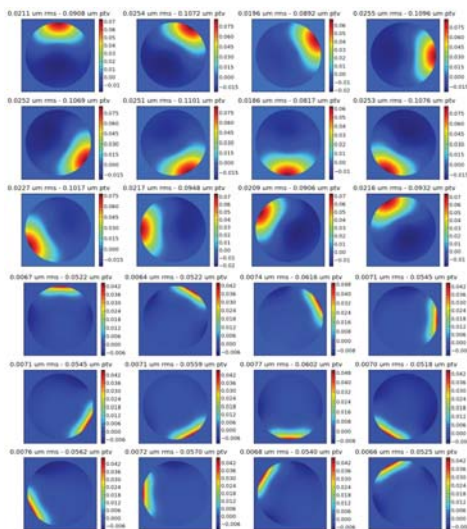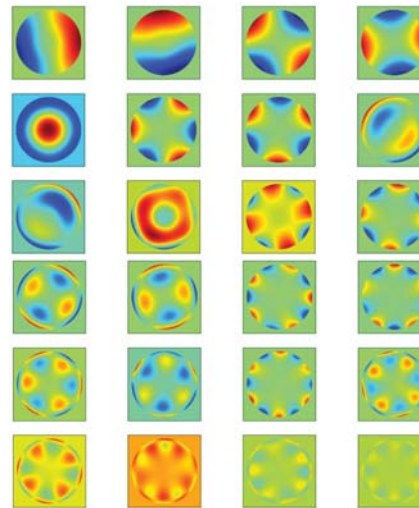

Fig. 5. System's Eigen Modes, sorted from the less to the more energetical, deduced from a Singular Value Decomposition of the measured IF base.

B. Expected correction performance

As explained in Section II-B, each specified mode, at its maximum amplitude, is projected on the measured IF base to determine the mirror correction capacity. As the IF are similar to the FEA results, the system performance are well recovered (Figure 6). All the modes are corrected with a precision better than 5 nm rms, except from the spherical and pentafoil which are slightly above. The residuals of spherical generation come from the central clamping and the residuals of pentafoil are due to the symmetry mismatch between the system and the mode.

The precision of correction of a representative Wave-Front Error (WFE) is deduced from these results. The WFE is defined as a random combination of the 9 Zernike modes, weighted by their maximum specified amplitude. In the worst case, the total residuals will be 11.1 nm rms, to be compared to the 10.2 nm rms expected from simulation. Then the mean precision of correction is determined by studying the correction of 1000 random WFE: 6.3 nm rms, with a standard deviation of 1.5 nm rms.

Fig. 3. Mirror's Influence Functions, measured with a Fizeau interferometer [μm].
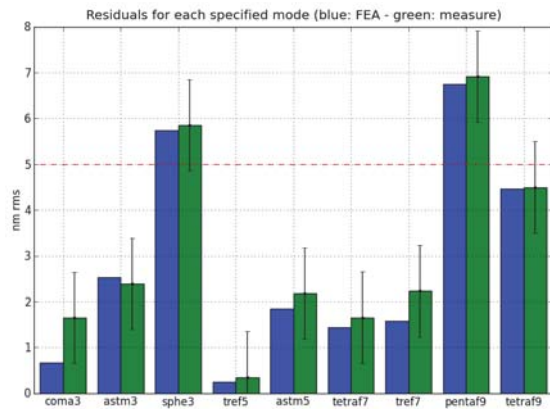
Fig. 6. Residual WFE computed for each specified modes, with simulated and measured IF (errorbars correspond to the interferometer precision: ± 1 nm).

C. Dead actuator study

With the knowledge of the Influence Functions, the impact of a dead actuator can be characterized. A dead actuator is defined as a free point: the piezoelectric is not supplied any more but as it has a certain stiffness, the actuation point will follow the deformation, which is less perturbing than a clamped point.

A dead actuator occurrence can be modeled in two different ways, depending if there is a system recalibration or not. Without recalibration, the mode to be corrected is still projected on the 24 IF but the command of the dead actuator is forced to 0 for the wave-front reconstruction. With a recalibration, the mode projection is done on the 23 remaining IF so the actuator absence will be compensated by its neighbors. This case being advantageous, we study it in more details.

The impact of a dead actuator will depend on the actuator location and on the mode to be corrected. The performance of correction is calculated for each mode and for each actuator, Figure 7 presents the mean resulting residuals and the worst and best cases, compared to the performance of the fully functional system. The loss of one actuator deteriorates the performance in a reasonable way: the correction stays within the specifications. Then the evolution of the mean correction performance with the number of dead actuators is studied: for a given number of dead actuators, 50 random sets of defective actuators are drawn and the correction of 100 random WFEs is performed for each deteriorated IF bases (Figure 7). Logically, the more there are dead actuators, the more the correction is damaged, but we can see that with 2 dead actuators the system is still well functioning: the mean precision is 10.7 nm rms, with a standard deviation of 2.1 nm rms. As a conclusion, we can say that such a system has an intrinsic redundancy: there are 24 actuators for 17 modes to correct. This fact, ensuring the system robustness and reliability, is really interesting and important for a space use.
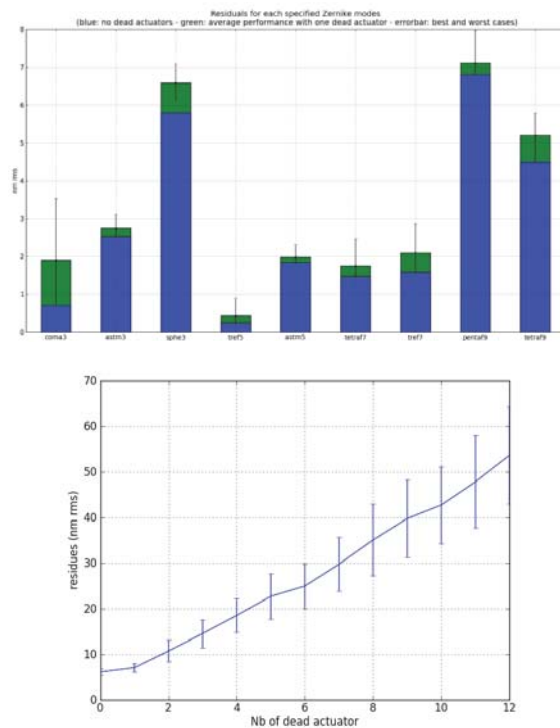

Fig. 7. System performance with dead actuators (FEA results): Top: comparison of the precision of correction of a system fully functionnal and a system with one dead actuator - Bottom: evolution of the mean expected residual wave-front with the number of dead actuator (each point is a statistic on 50 random sets of dead actuators and 100 random WFE for each set).

IV. ACTIVE LOOP PERFORMANCE

A. Test bed design

With the interferometrical tests, simulated and measured performance have been correlated. The mirror is then tested in a representative configuration, to validate its functioning in closed loop. The test bed is composed of a telescope simulator and the active correction loop. Shack-Hartmann wave-front sensing and imaging Point Spread Function will allow a complete validation of the mirror in term of wave-front precision. While functioning, the mirror deformation is monitored with the Fizeau interferometer and force sensors on the actuators will validate the system mechanical behavior.

The telescope simulator is an adaptive optics loop with a 88-actuators Deformable Mirror (DM) and a Shack-Hartmann wave-front sensor (WFS). This first DM defines the entrance pupil plane, it simulates the telescope primary mirror and its deformations. This loop injects calibrated Wave-Front Errors on MADRAS mirror, which is conjugated to the first DM. The active correction loop is composed of the MADRAS mirror, a second Shack-Hartmann WFS and a Real Time Computer which analyzes the measured wave-front and commands the mirror in order to converge to a plane wave-front. Two cameras, located in image plans before and after the correction, allow characterizing the correction effects on the PSF.
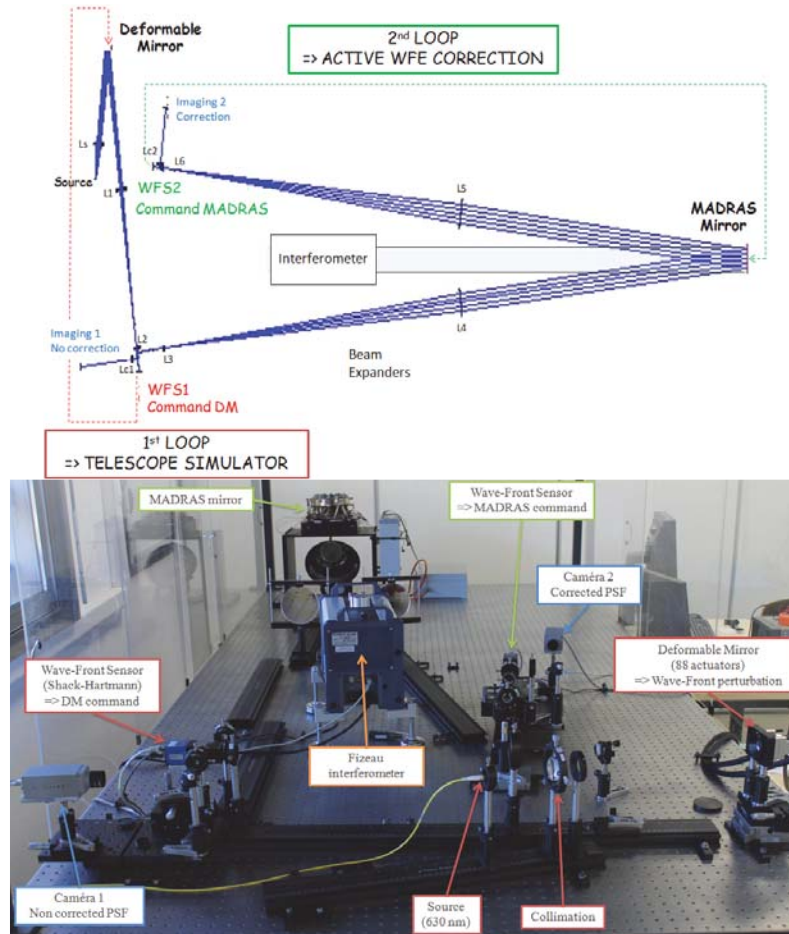
Fig. 8.   MADRAS test-bed: optical design and picture.

B. Calibration

The precision of the wave-front injected on our test-bed with the first loop simulating the telescope has been characterized with wave-front measurements: flat wave-front and specified Zernike modes are generated with a residual error of 5 nm rms.

The active system calibration consists in performing an inter-action matrix: the influence function are measured with the wave-front sensor in order to compute a command matrix. To simulate the external handling of tip, tilt and focus, three virtual influence functions, corresponding to these three modes are added to the interaction matrix.

The loop noise is characterized by correcting the turbulent phase: a wave-front error is measured at $\pm$ 3.4 nm rms. This precision is reduced to $\pm$ 0.5 nm rms by averaging 50 measurements.

Due to the actuators integration, MADRAS optical surface contains shape errors, inducing a WFE of 200 nm rms, mainly composed of focus, astigmatism and coma. Moreover, there are some aberrations in the optical path, due to misalignment, inducing a WFE of 18 nm rms. For an efficient PSF mea-surement, the first step is to correct these WFEs seen by the Wave-Front Sensor. This flattening is obtained with an error of 12.2 nm rms (see Figure 9). This residual wave-front will then be the target for the next corrections.
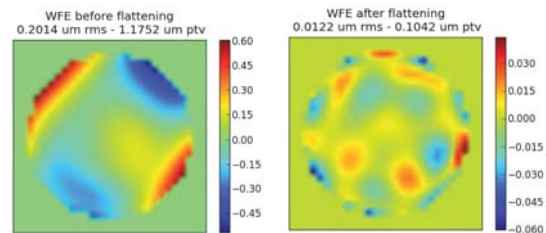

Fig. 9.   WFE before and after flattening (tip, tilt and focus substracted).

C. Mode correction

Once the reference taken and the test-bed characterized, we send the specified Zernike mode with the generation loop and we study the correction with the MADRAS system. The measured performance, presented on the left of 10, are really satisfactory: the expected precision of correction are recovered for most of the modes.
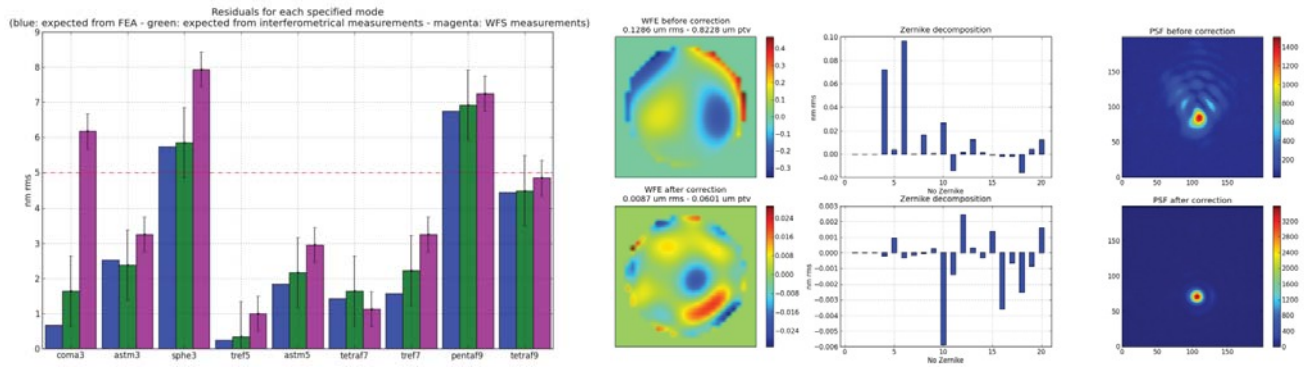
Fig. 10. Closed loop MADRAS performance: Left: mode correction, compared to expected performance (errorbars correspond to the interferometer and ASO precisions) - Right: Correction of a random WFE (the given wave-front is an average of 100 measurements, tip, tilt and focus subtracted).

Coma and Spherical are less well corrected, due to filtering in the command matrix. The mathematical expression of coma is linked to tilt, and our method to filter this mode probably impact the coma correction. The same problem appears with the focus filtering, impacting the spherical correction. We are currently investigating other methods to define our command matrix in order to improve the performance.

In conclusion, all of the specified Zernike modes are corrected with a precision better than 8 nm rms. As expected from simulations, the correction of Astigmatism3&5, Trefoil5&7 and Tetrafoil7&9 is efficient, with a precision below 5 nm rms, and Pentafoil9 correction precision is around 7 nm rms. Coma and Spherical are currently corrected with a precision of respectively 6 and 8 nm rms, it will be improved by working on the command matrix.

D. Representative wave-front error correction

After having demonstrated the system capacity to correct each specified modes separately, we generate a more representative WFE. The correction of a random combination of the specified modes will validate the system's linearity and its correction performance regarding the deformation expected in space telescope.

Figure 10, right, presents a correction case with the injected wave-front error, the residual wave-front after correction and the corresponding PSFs. The gain for the PSF measurement is obvious and, with a residual wave-front of 8.7 ± 0.5 nm rms, we are within the 10 nm rms precision specification.

The mirror behavior is linear: if the injected WFE is a combination of Zernike modes, $\phi_{in} = \sum_i A_i Z_i$, the residual wave-front ϕ_{res} can be deduced from each specified modes measured precision of correction ($\phi_{res,i}$, presented in Figure 10):

$$\phi_{res} = \sqrt{\sum_i \left(\frac{A_{spec,i} \phi_{res,i}}{A_i} \right)^2}, \qquad (6)$$

with $A_{spec,i}$ the maximum amplitude specified for each mode. Thus, a statistical study on 1000 random WFEs is performed, giving the mean residual wave-front after correction.

MADRAS system is able to compensate for the deformations expected in space telescopes with a mean precision of 9.0 nm rms, with a standard deviation of 1.8 nm rms.

V. Conclusion and perspectives

MADRAS project has been initiated to demonstrate the possibility and the interest of inserting a correcting active mirror in the next generation of space telescope. The chosen design allow an efficient correction of 17 Zernike polynomials with only 24 actuators. The mirror is in Zerodur and its supporting system in Invar. It is light (4 kg) and small (80 mm high and 130 mm diameter). Such a design has been optimized with Finite Element Analysis in order to ensure the correction performance but also the mechanical strength and the system survival in launch and space environments. The correcting system has been realized and tested, demonstrating its capacity to compensate for large lightweight primary mirrors in space. We have shown a really good match between simulation and measurement, validating the design method. The first experimental results demonstrate promising correction performance: most of the modes are individually corrected with a precision of 5 nm rms and statistical analysis of the correction of random representative WFEs gives the mean precision of correction around 10 nm rms. A study on the dead actuator has shown that the system performance are not too much impacted by the loss of 2 actuators. This redundancy is interesting for the system reliability and robustness.

With piezoelectric actuators, it is important to work in closed loop but if needed, the actuator technology could be changed in order to converge to the required mirror shape in only one iteration.

With this project, the presented deformable mirror technology has reached a Technology Readiness Level 4. The next step is then the TRL5 with a validation in space environment.

Acknowledgment

REFERENCES

[1] P. Murdin, Ed., *Active Optics*. Encyclopedia of Astronomy and Astrophysics, Nov. 2000.

[2] R. H. Freeman and J. E. Pearson, "Deformable mirrors for all seasons and reasons," *Applied Optics*, vol. 21, pp. 580–588, Feb. 1982.

[3] R. N. Wilson, F. Franza, and L. Noethe, "Active optics. I. A system for optimizing the optical quality and reducing the costs of large telescopes." *J. Mod. Opt., Vol. 34, No. 4, p. 485 - 509*, vol. 34, pp. 485–509, 1987.

[4] M. Ferrari, "Development of a variable curvature mirror for the delay lines of the VLT interferometer," *Astronomy and Astrophysics*, vol. 128, pp. 221–227, Feb. 1998.

[5] J. Lubliner and J. E. Nelson, "Stressed mirror polishing. 1: A technique for producing nonaxisymmetric mirrors," *Applied Optics*, vol. 19, pp. 2332–+, Jul. 1980.

[6] L. Feinberg, L. Cohen, B. Dean, W. Hayden, J. Howard, and R. Keski-Kuha, "Space telescope design considerations," *Optical Engineering*, vol. 51, no. 1, p. 011006, Jan. 2012.

[7] M. Postman, T. Brown, K. Sembach, M. Giavalisco, W. Traub, K. Stapelfeldt, D. Calzetti, W. Oegerle, R. Michael Rich, H. Phillip Stahl, J. Tumlinson, M. Mountain, R. Soummer, and T. Hyde, "Advanced Technology Large-Aperture Space Telescope: science drivers and technology developments," *Optical Engineering*, vol. 51, no. 1, p. 011007, Jan. 2012.

[8] P. A. Lightsey, C. Atkinson, M. Clampin, and L. D. Feinberg, "James Webb Space Telescope: large deployable cryogenic telescope in space," *Optical Engineering*, vol. 51, no. 1, p. 011003, Jan. 2012.

[9] K. Patterson, N. Yamamoto, and S. Pellegrino, "Thin deformable mirrors for a reconfigurable space telescope," ser. 53rd AIAA Structures, Structural Dynamics, and Materials Conference, 2012.

[10] B. K. McComas, "Configurable adaptive optics for the correction of space-based optical systems," Ph.D. dissertation, University of Colorado at Boulder, 2002.

[11] D. Redding, D. Coulter, and J. Wellman, "Active Optics for Low-Cost Astronomical Space Telescopes," in *American Astronomical Society Meeting Abstracts*, ser. American Astronomical Society Meeting Abstracts, vol. 219, Jan. 2012, p. 136.05.

[12] L. E. Cohan and D. W. Miller, "Integrated modeling for design of lightweight, active mirrors," *Optical Engineering*, vol. 50, no. 6, pp. 063 003–+, Jun. 2011.

[13] G. R. Lemaître, "Active Optics: Vase or Meniscus Multimode Mirrors and Degenerated Monomode Configurations," *Meccanica*, vol. 40, pp. 233–249, 2005.

[14] R. J. Noll, "Zernike polynomials and atmospheric turbulence," *Journal of the Optical Society of America (1917-1983)*, vol. 66, pp. 207–211, Mar. 1976.

[15] S. P. Timoshenko and S. Woinowsky-Krieger, *Theory of Plates and Shells*, ser. Engineering Mechanics Series. McGRAW-Hill International Editions, 1959.

[16] T. Döhring, R. Jedamzik, A. Thomas, and P. Hartmann, "Forty years of ZERODUR mirror substrates for astronomy: review and outlook," in *Society of Photo-Optical Instrumentation Engineers (SPIE) Conference Series*, ser. Society of Photo-Optical Instrumentation Engineers (SPIE) Conference Series, vol. 7018, Jul. 2008.

[17] C. Paterson, I. Munro, and J. C. Dainty, "A low cost adaptive optics system using a membrane mirror," *Optics Express*, vol. 6, pp. 175–+, Apr. 2000.